

First Observation of the Decays $B^0 \rightarrow D^{*-} p \bar{p} \pi^+$ and $B^0 \rightarrow D^{*-} p \bar{n}$

S. Anderson,¹ V. V. Frolov,¹ Y. Kubota,¹ S. J. Lee,¹ R. Mahapatra,¹ J. J. O'Neill,¹ R. Poling,¹ T. Riehle,¹ A. Smith,¹ C. J. Stepaniak,¹ J. Urheim,¹ S. Ahmed,² M. S. Alam,² S. B. Athar,² L. Jian,² L. Ling,² M. Saleem,² S. Timm,² F. Wappler,² A. Anastasov,³ J. E. Duboscq,³ E. Eckhart,³ K. K. Gan,³ C. Gwon,³ T. Hart,³ K. Honscheid,³ D. Hufnagel,³ H. Kagan,³ R. Kass,³ T. K. Pedlar,³ H. Schwarthoff,³ J. B. Thayer,³ E. von Toerne,³ M. M. Zoeller,³ S. J. Richichi,⁴ H. Severini,⁴ P. Skubic,⁴ A. Undrus,⁴ S. Chen,⁵ J. Fast,⁵ J. W. Hinson,⁵ J. Lee,⁵ D. H. Miller,⁵ E. I. Shibata,⁵ I. P. J. Shipsey,⁵ V. Pavlunin,⁵ D. Cronin-Hennessy,⁶ A. L. Lyon,⁶ E. H. Thorndike,⁶ C. P. Jessop,⁷ H. Marsiske,⁷ M. L. Perl,⁷ V. Savinov,⁷ X. Zhou,⁷ T. E. Coan,⁸ V. Fadeyev,⁸ Y. Maravin,⁸ I. Narsky,⁸ R. Stroynowski,⁸ J. Ye,⁸ T. Wlodek,⁸ M. Artuso,⁹ R. Ayad,⁹ C. Boulahouache,⁹ K. Bukin,⁹ E. Dambasuren,⁹ S. Karamov,⁹ G. Majumder,⁹ G. C. Moneti,⁹ R. Mountain,⁹ S. Schuh,⁹ T. Skwarnicki,⁹ S. Stone,⁹ G. Viehhauser,⁹ J. C. Wang,⁹ A. Wolf,⁹ J. Wu,⁹ S. Kopp,¹⁰ A. H. Mahmood,¹¹ S. E. Csorna,¹² I. Danko,¹² K. W. McLean,¹² Sz. Márka,¹² Z. Xu,¹² R. Godang,¹³ K. Kinoshita,^{13,*} I. C. Lai,¹³ S. Schrenk,¹³ G. Bonvicini,¹⁴ D. Cinabro,¹⁴ S. McGee,¹⁴ L. P. Perera,¹⁴ G. J. Zhou,¹⁴ E. Lipeles,¹⁵ S. P. Pappas,¹⁵ M. Schmidtler,¹⁵ A. Shapiro,¹⁵ W. M. Sun,¹⁵ A. J. Weinstein,¹⁵ F. Würthwein,^{15,†} D. E. Jaffe,¹⁶ G. Masek,¹⁶ H. P. Paar,¹⁶ E. M. Potter,¹⁶ S. Prell,¹⁶ V. Sharma,¹⁶ D. M. Asner,¹⁷ A. Eppich,¹⁷ T. S. Hill,¹⁷ R. J. Morrison,¹⁷ R. A. Briere,¹⁸ G. P. Chen,¹⁸ B. H. Behrens,¹⁹ W. T. Ford,¹⁹ A. Gritsan,¹⁹ J. Roy,¹⁹ J. G. Smith,¹⁹ J. P. Alexander,²⁰ R. Baker,²⁰ C. Bebek,²⁰ B. E. Berger,²⁰ K. Berkelman,²⁰ F. Blanc,²⁰ V. Boisvert,²⁰ D. G. Cassel,²⁰ M. Dickson,²⁰ P. S. Drell,²⁰ K. M. Ecklund,²⁰ R. Ehrlich,²⁰ A. D. Foland,²⁰ P. Gaidarev,²⁰ L. Gibbons,²⁰ B. Gittelman,²⁰ S. W. Gray,²⁰ D. L. Hartill,²⁰ B. K. Heltsley,²⁰ P. I. Hopman,²⁰ C. D. Jones,²⁰ J. Kandaswamy,²⁰ D. L. Kreinick,²⁰ M. Lohner,²⁰ A. Magerkurth,²⁰ T. O. Meyer,²⁰ N. B. Mistry,²⁰ E. Nordberg,²⁰ J. R. Patterson,²⁰ D. Peterson,²⁰ D. Riley,²⁰ J. G. Thayer,²⁰ D. Urner,²⁰ B. Valant-Spaight,²⁰ A. Warburton,²⁰ P. Avery,²¹ C. Prescott,²¹ A. I. Rubiera,²¹ J. Yelton,²¹ J. Zheng,²¹ G. Brandenburg,²² A. Ershov,²² Y. S. Gao,²² D. Y.-J. Kim,²² R. Wilson,²² T. E. Browder,²³ Y. Li,²³ J. L. Rodriguez,²³ H. Yamamoto,²³ T. Bergfeld,²⁴ B. I. Eisenstein,²⁴ J. Ernst,²⁴ G. E. Gladding,²⁴ G. D. Gollin,²⁴ R. M. Hans,²⁴ E. Johnson,²⁴ I. Karliner,²⁴ M. A. Marsh,²⁴ M. Palmer,²⁴ C. Plager,²⁴ C. Sedlack,²⁴ M. Selen,²⁴ J. J. Thaler,²⁴ J. Williams,²⁴ K. W. Edwards,²⁵ R. Janicek,²⁶ P. M. Patel,²⁶ A. J. Sadoff,²⁷ R. Ammar,²⁸ A. Bean,²⁸ D. Besson,²⁸ R. Davis,²⁸ N. Kwak,²⁸ and X. Zhao²⁸

(CLEO Collaboration)

¹University of Minnesota, Minneapolis, Minnesota 55455

²State University of New York at Albany, Albany, New York 12222

³Ohio State University, Columbus, Ohio 43210

⁴University of Oklahoma, Norman, Oklahoma 73019

⁵Purdue University, West Lafayette, Indiana 47907

⁶University of Rochester, Rochester, New York 14627

⁷Stanford Linear Accelerator Center, Stanford University, Stanford, California 94309

⁸Southern Methodist University, Dallas, Texas 75275

⁹Syracuse University, Syracuse, New York 13244

¹⁰University of Texas, Austin, Texas 78712

¹¹University of Texas—Pan American, Edinburg, Texas 78539

¹²Vanderbilt University, Nashville, Tennessee 37235

¹³Virginia Polytechnic Institute and State University, Blacksburg, Virginia 24061

¹⁴Wayne State University, Detroit, Michigan 48202

¹⁵California Institute of Technology, Pasadena, California 91125

¹⁶University of California, San Diego, La Jolla, California 92093

¹⁷University of California, Santa Barbara, California 93106

¹⁸Carnegie Mellon University, Pittsburgh, Pennsylvania 15213

¹⁹University of Colorado, Boulder, Colorado 80309-0390

²⁰Cornell University, Ithaca, New York 14853

²¹University of Florida, Gainesville, Florida 32611

²²Harvard University, Cambridge, Massachusetts 02138

²³University of Hawaii at Manoa, Honolulu, Hawaii 96822

²⁴University of Illinois, Urbana-Champaign, Illinois 61801

²⁵Carleton University, Ottawa, Ontario, Canada K1S 5B6

and the Institute of Particle Physics, Canada

²⁶McGill University, Montréal, Québec, Canada H3A 2T8
 and the Institute of Particle Physics, Canada
²⁷Ithaca College, Ithaca, New York 14850
²⁸University of Kansas, Lawrence, Kansas 66045
 (Received 5 September 2000)

We report the first observation of exclusive decays of the type $B \rightarrow D^* N \bar{N} X$, where N is a nucleon. Using a sample of $9.7 \times 10^6 B \bar{B}$ pairs collected with the CLEO detector operating at the Cornell Electron Storage Ring, we measure the branching fractions $\mathcal{B}(B^0 \rightarrow D^{*-} p \bar{p} \pi^+) = (6.5^{+1.3}_{-1.2} \pm 1.0) \times 10^{-4}$ and $\mathcal{B}(B^0 \rightarrow D^{*-} p \bar{n}) = (14.5^{+3.4}_{-3.0} \pm 2.7) \times 10^{-4}$. Antineutrons are identified by their annihilation in the CsI electromagnetic calorimeter.

DOI: 10.1103/PhysRevLett.86.2732

PACS numbers: 13.25.Hw, 14.40.Nd

A unique feature of the B meson system is that the large mass of the b quark allows for many of the weak decays of the B meson to include the creation of a baryon-antibaryon pair. In the simplest picture, baryons are expected to be produced in decays of the type $B \rightarrow \bar{\Lambda}_c p X$, and it has been only decays of this type which have been exclusively reconstructed to date [1]. However, one can combine the recently measured value $\mathcal{B}(\Lambda_c^+ \rightarrow p K^- \pi^+) = (5.0 \pm 0.5 \pm 1.2)\%$ [2] with estimates of the product branching fraction $\mathcal{B}(B \rightarrow \Lambda_c X) \times \mathcal{B}(\Lambda_c \rightarrow p K^- \pi^+)$ of $(1.81 \pm 0.22 \pm 0.24) \times 10^{-3}$ [3] to determine that $B \rightarrow \bar{\Lambda}_c N X$ modes, where N is a proton or a neutron, account for only about half of the total $B \rightarrow \text{baryons}$ rate. Dunietz [4] has suggested that modes of the type $B \rightarrow D N \bar{N} X$, in which D represents any charmed meson, are likely to be sizable. $B \rightarrow D N \bar{N} X$ final states can arise from either the hadronization of the W boson into a baryon-antibaryon pair, or the production of a highly excited charmed baryon which decays strongly into a baryon plus a charmed meson. CLEO has previously reported an inclusive upper limit for $\mathcal{B}(B \rightarrow D N \bar{N} X)$ of $<4.8\%$ at 90% C.L. [5]. We report the first observation of decays of this type, and present measurements of the branching fractions $\mathcal{B}(B^0 \rightarrow D^{*-} p \bar{p} \pi^+)$ and $\mathcal{B}(B^0 \rightarrow D^{*-} p \bar{n})$. These branching fractions are substantial, indicating that the decays are an important component of B decays and need to be included in the modeling of B decays used in the study of many different processes. The charge conjugate process is implied in the reconstruction of $B^0 \rightarrow D^{*-} p \bar{p} \pi^+$. However, in the reconstruction of $B^0 \rightarrow D^{*-} p \bar{n}$ only the mode with the antineutron is used in our measurement because neutrons do not have a distinctive annihilation signature in the CLEO detector. Further details of this analysis may be obtained elsewhere [6].

The data were taken with the CLEO II detector [7] at the Cornell Electron Storage Ring (CESR). The sample we use corresponds to an integrated luminosity of 9.1 fb^{-1} from data taken on the $Y(4S)$ resonance, corresponding to $9.7 \times 10^6 B \bar{B}$ pairs, and 4.5 fb^{-1} in the continuum at energies just below the $Y(4S)$. We assume that 50% of the $B \bar{B}$ pairs consist of $B^0 \bar{B}^0$, and that there are equal numbers of B^0 and \bar{B}^0 mesons. Charged particle trajectories are measured in a cylindrical drift chamber operating in a 1.5 T magnetic field. Photons and antineutrons are de-

tected using a calorimeter consisting of 7800 CsI crystals with excellent resolution in position and electromagnetic shower energy. Simulated events were generated with a GEANT-based Monte Carlo program [8]. Sixty percent of the data were taken in the CLEO II.V configuration [9].

Charged particle identification is accomplished by combining the specific ionization (dE/dx) measurements from the drift chamber with time-of-flight (TOF) scintillation counter measurements. We reconstruct the decay mode $D^{*-} \rightarrow \bar{D}^0 \pi^-$, with $\bar{D}^0 \rightarrow K^+ \pi^-$, $\bar{D}^0 \rightarrow K^+ \pi^- \pi^0$, and $\bar{D}^0 \rightarrow K^+ \pi^- \pi^+ \pi^-$. Pairs of calorimeter showers with photonlike lateral shower shapes and invariant mass within 2.5 standard deviations of $M(\pi^0)$ are considered as π^0 candidates. We select D^{*-} candidates using 95% efficient cuts around the central values of the M_{D^0} and $(M_{D^*} - M_{D^0})$ distributions. The resolution in these distributions was found from the Monte Carlo program for each of the 3 decay modes and 2 datasets. This led to cuts varying from ± 12 to ± 27 MeV around the D^0 mass, and from ± 0.9 to ± 1.5 MeV around the D^* mass. Examples of M_{D^0} and $M(M_{D^*} - M_{D^0})$ distributions from B decays at CLEO can be found elsewhere [10]. In the few cases where there is more than one D^* candidate in an event, the candidate which is closest to $M_{D^0} = 1.8646$ GeV and $(M_{D^*} - M_{D^0}) = 0.1454$ GeV [11] is chosen.

To reconstruct B^0 candidates for $B^0 \rightarrow D^{*-} p \bar{p} \pi^+$, we calculate the beam constrained mass, $M(B) \equiv \sqrt{E_{\text{beam}}^2 - p(B)^2}$, where E_{beam} is the beam energy, and $p(B)$ is the B^0 candidate three-momentum magnitude. We also use the energy difference between the beam energy and the energy of the reconstructed B candidate: $\Delta E \equiv E_{\text{beam}} - E(B)$. Using a Monte Carlo simulation program, we find the detector resolution for the ΔE distribution for each D^0 mode, and require that the measured ΔE is within 3 standard deviations of zero.

The $M(B)$ resolution is dominated by the beam energy spread and is consistent with the Monte Carlo simulation for $B^0 \rightarrow D^{*-} p \bar{p} \pi^+$, which predicts it to be Gaussian with a width of $\sigma = 2.7$ MeV. The $M(B)$ distribution is fitted to a Gaussian function with the predicted width, and a polynomial background function with suppression at the E_{beam} threshold. The fitted signal yield is $32.3^{+6.3}_{-6.0}$ events, where the errors are statistical only. If σ is allowed to float, a value of $\sigma = 2.1 \pm 0.4$ MeV is obtained, consistent

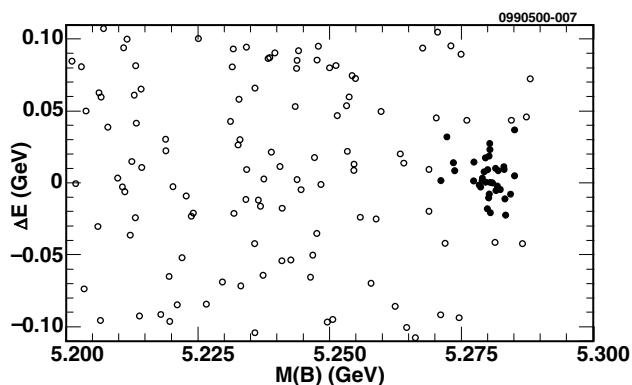


FIG. 1. ΔE vs $M(B)$ distribution for $B^0 \rightarrow D^{*-} p \bar{p} \pi^+$. The solid circles indicate events in the signal region.

with the Monte Carlo prediction. Figure 1 shows ΔE vs $M(B)$ for $B^0 \rightarrow D^{*-} p \bar{p} \pi^+$, and Fig. 2(a) shows $M(B)$ for $B^0 \rightarrow D^{*-} p \bar{p} \pi^+$.

To find the decay $B^0 \rightarrow D^{*-} p \bar{n}$ requires the detection of an antineutron. This is accomplished by identifying annihilation showers in the CsI calorimeter. Antiprotons and antineutrons annihilate with nucleons in the calorimeter. These annihilations result in showers with different characteristics than those from photons or charged particles. We use antiproton annihilation showers to define the antineutron selection criteria since we are unable to isolate a sample of antineutrons in data. Our antiproton sample consists of 1.6×10^5 \bar{p} 's from reconstructed $\bar{\Lambda} \rightarrow \bar{p} \pi^+$ decays, in which the daughter antiprotons are selected by dE/dx and TOF response. The isolation of this sample is independent of calorimeter response and therefore allows

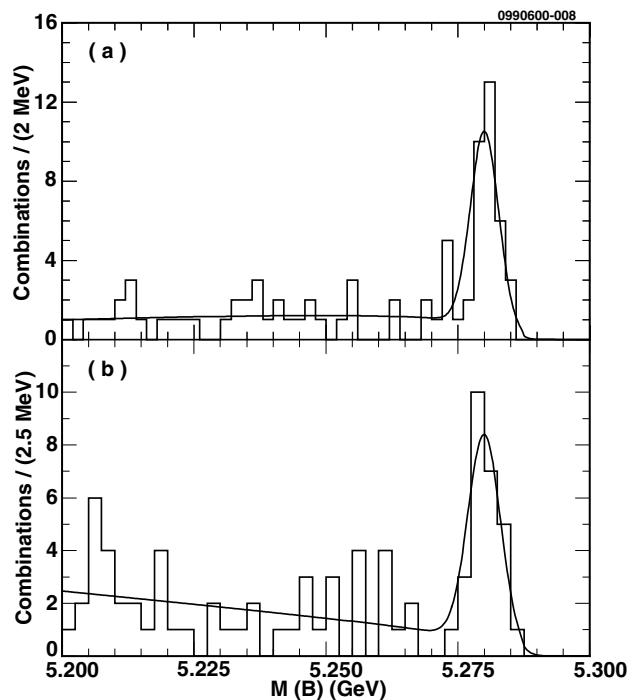


FIG. 2. $M(B)$ distribution for (a) $B^0 \rightarrow D^{*-} p \bar{p} \pi^+$ and (b) $B^0 \rightarrow D^{*-} p \bar{n}$. Each plot is fitted to the sum of a background function and a fixed-width Gaussian signal shape.

us to evaluate our shower-based selection criteria. Based upon Monte Carlo simulations, we expect these same criteria to be effective for isolating antineutron candidates.

We find that antineutrons typically deposit a substantial amount of energy in a laterally broad shower, which has energy E_{main} , and a lesser amount of energy in adjacent satellite showers, whose energy is added to E_{main} to define E_{group} . The selection of showers with $E_{\text{main}} > 500$ MeV and $E_{\text{group}} > 800$ MeV is useful in suppressing backgrounds, while retaining many antineutron annihilation showers. The main shower must have polar angle θ with respect to the incoming positron direction of $45^\circ < \theta < 135^\circ$ to ensure that it is located in that part of the calorimeter that has the best resolution, must have a lateral shape broader than typical photons, and must not match the projection of any charged track trajectory. Baryon number conservation serves as an added background suppressant: once we require that there be a proton, the likelihood of an annihilationlike shower in the event to be an antineutron increases significantly. The reconstruction efficiency as a function of momentum for antineutrons in a Monte Carlo sample of $B^0 \rightarrow D^{*-} p \bar{n}$ events in which the B^0 selection criteria have been applied is shown in Figure 3.

The measured shower energy for an antineutron, E_{group} , does not give an accurate measurement of the total energy of the antineutron. We therefore assign the energy of the antineutron candidate using $E(\bar{n}) = E_{\text{beam}} - E(D^{*-}) - E(p)$. We then use this energy, together with the position of the antineutron shower, to calculate the momentum of the antineutron candidate. This momentum is added to the momenta of the D^{*-} and p candidates to give the momentum of the B^0 meson, $p(B)$. The B^0 candidate mass is then calculated with $M(B) = \sqrt{E_{\text{beam}}^2 - p(B)^2}$.

The mass resolution of the reconstructed B^0 meson is estimated from a Monte Carlo simulation to be Gaussian with a width $\sigma = 3.1$ MeV, demonstrating that the lack of a direct measurement of the antineutron energy does not seriously degrade the $M(B)$ resolution relative to $B^0 \rightarrow D^{*-} p \bar{p} \pi^+$. However, for this mode we cannot use the requirement that ΔE is consistent with zero, as we do not have two independent measures of the energy of the B^0 .

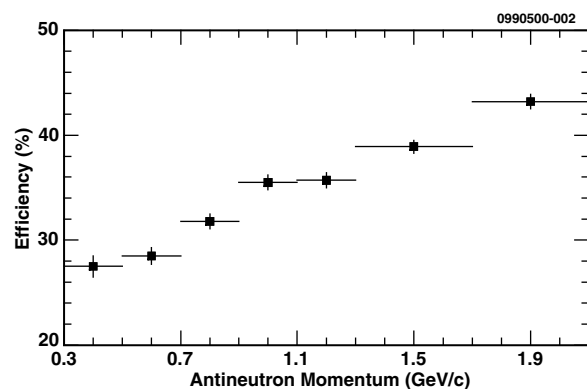


FIG. 3. Antineutron reconstruction efficiency derived from simulated $B^0 \rightarrow D^{*-} p \bar{n}$ events.

In reconstructing $B^0 \rightarrow D^{*-} p \bar{n}$ we could also be reconstructing $B^0 \rightarrow D^{*-} D_s^+$ with $D_s^+ \rightarrow p \bar{n}$. This latter decay has not been observed but could occur via $c\bar{s}$ annihilation. We might also be including events that are $B^0 \rightarrow D^{*-} D_s^{*+}$ with $D_s^{*+} \rightarrow D_s^+ \gamma$ or $D_s^{*+} \rightarrow D_s^+ \pi^0$ and $D_s^+ \rightarrow p \bar{n}$. These events will populate the $M(B)$ signal region but with a broader signal peak due to the missing soft photon or π^0 . We eliminate these two types of decay by rejecting events with $1.91 < M(p\bar{n})$ (GeV) < 2.04 GeV, for a loss of only 9% in the relative reconstruction efficiency.

The final data $M(B)$ distribution, shown in Fig. 2(b), is fit with a Monte Carlo predicted Gaussian width of $\sigma = 3.1$ MeV and gives a signal yield of $24.0^{+5.6}_{-5.0}$ events. If σ is allowed to float, a value of 2.6 ± 0.4 MeV is found, consistent with the Monte Carlo expectation.

We use a Monte Carlo simulation to calculate detection efficiencies to be 0.52% for $B^0 \rightarrow D^{*-} p \bar{p} \pi^+$, and 0.34% for $B^0 \rightarrow D^{*-} p \bar{n}$, where these numbers include all the relevant branching fractions of the daughters. The Monte Carlo generation of the decays assume no resonant substructure. No evidence of substructure has been found in the signal candidates. However, we will allow for the possibility of substructure, which would alter the efficiency, in our estimation of the systematic uncertainties.

Whereas the Monte Carlo simulation has been well tested for charged particles and photons, this is the first measurement that has explicitly needed the efficiency for antinucleon annihilations in the calorimeter. We find a discrepancy for antiproton annihilation showers between the Monte Carlo and data. The reconstruction efficiency for Monte Carlo and data for antiprotons, as determined from the aforementioned $\bar{\Lambda}$ sample, is shown in Fig. 4(a). We find that the antiproton reconstruction efficiency is overestimated by the GEANT simulation prediction. Since the electromagnetic interactions of the antiproton are expected to be well simulated by GEANT, we attribute the discrepancy to imperfect modeling of the annihilation in CsI and scale down the Monte Carlo antineutron efficiency by the same relative factor found for antiprotons. Weighting the efficiency correction for antiprotons by the expected antineutron momentum spectrum results in an antineutron selection efficiency which is 21% lower than the GEANT Monte Carlo simulation. Possible inaccuracy in this estimate of the correction factor is accounted for in the systematic uncertainty. In Fig. 4(b) we show the antineutron momentum spectrum generated in Monte Carlo for $B \rightarrow D^{*-} p \bar{n}$ decays.

We search for, but do not find, resonant substructure contributions to $B^0 \rightarrow D^{*-} p \bar{p} \pi^+$ and $B^0 \rightarrow D^{*-} p \bar{n}$ decays. Examples of possible substructure arise from a heavy charmed baryon decaying strongly to $(\bar{p} D^{*-})$ for $B^0 \rightarrow D^{*-} p \bar{p} \pi^+$ and $(\bar{n} D^{*-})$ for $B^0 \rightarrow D^{*-} p \bar{n}$, and a resonance of the virtual W decaying to $p \bar{p} \pi^+$. We also study the effect on the Monte Carlo reconstruction efficiency of a two-body decay into $D^{*-} X$, and find no evidence from the kinematic distribution of the daughter

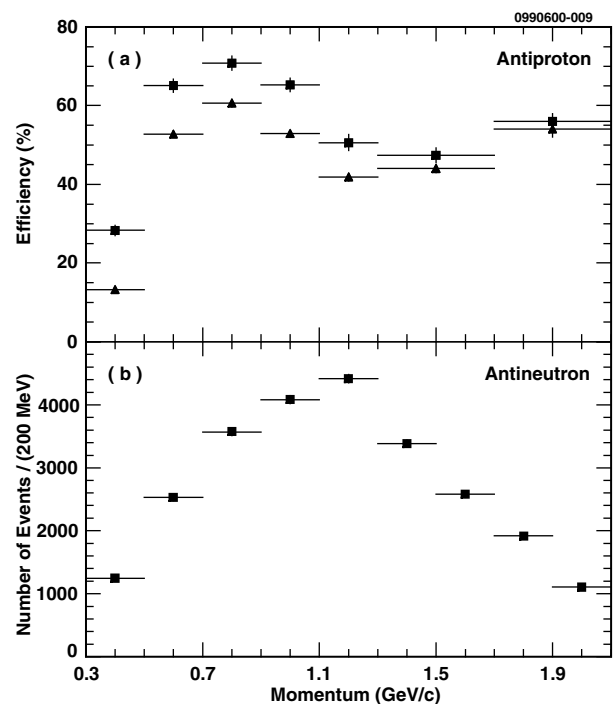


FIG. 4. (a) Antiproton reconstruction efficiency. Squares represent Monte Carlo efficiency and triangles that of the data. (b) Monte Carlo antineutron momentum spectrum in simulated $B^0 \rightarrow D^{*-} p \bar{n}$ decays.

particles for decays of this type. We also find insignificant background from B decays with a charmed baryon final state or from other $B \rightarrow D^{*-} X$ modes.

We have considered many sources of systematic uncertainty of these branching fraction measurements. Systematic uncertainties shared by both modes are statistical uncertainty of D^0 branching fractions (0.6%) and D^{*-} branching fraction (1.4%), D^{*-} reconstruction due to kinematic fitting and particle identification (5.0%), and Monte Carlo statistics (5.0%). Systematic uncertainties which differ for the two modes, and which we quote in parenthesis for $B^0 \rightarrow D^{*-} p \bar{p} \pi^+$ and $B^0 \rightarrow D^{*-} p \bar{n}$, respectively, are as follows: tracking, 1% per track (6.6%, 4.6%), proton identification criteria (8%, 4%), and n body versus two body for decay kinematics (5%, 3%). No statistically significant Δ baryon contribution to the $D^{*-} p \bar{p} \pi^+$ yield was found. We place a systematic uncertainty due to a possible Δ baryon contribution to the $B^0 \rightarrow D^{*-} p \bar{p} \pi^+$ signal. Also, we assign a 5% uncertainty on the yield of $B^0 \rightarrow D^{*-} p \bar{n}$ due to the possibility of Δ baryons with a missing π distorting the background shape in this mode. The systematic uncertainty for antineutron identification is estimated to be 15%, dominated by the uncertainties in the calculated efficiency correction factor. The quadrature sum of all systematic uncertainties is 15% for $B^0 \rightarrow D^{*-} p \bar{p} \pi^+$, and 19% for $B^0 \rightarrow D^{*-} p \bar{n}$.

In conclusion, we have made the first observation of decay modes of the B^0 of the type $B \rightarrow DN\bar{N}X$. As our measurements comprise only two of the many different final states of this type, they imply that $DN\bar{N}X$ final

states may contribute substantially to the total observed $B \rightarrow \text{baryons}$ rate. We measure the branching fractions $\mathcal{B}(B^0 \rightarrow D^{*-} p \bar{p} \pi^+) = (6.5_{-1.2}^{+1.3} \pm 1.0) \times 10^{-4}$, and $\mathcal{B}(B^0 \rightarrow D^{*-} p \bar{n}) = (14.5_{-3.0}^{+3.4} \pm 2.7) \times 10^{-4}$.

We gratefully acknowledge the effort of the CESR staff in providing us with excellent luminosity and running conditions. This work was supported by the National Science Foundation, the U.S. Department of Energy, the Research Corporation, the Natural Sciences and Engineering Research Council of Canada, the A.P. Sloan Foundation, the Swiss National Science Foundation, and the Alexander von Humboldt Stiftung.

*Permanent address: University of Cincinnati, Cincinnati, Ohio 45221.

†Permanent address: Massachusetts Institute of Technology, Cambridge, Massachusetts 02139.

- [1] CLEO Collaboration, X. Fu *et al.*, Phys. Rev. Lett. **79**, 3125 (1997).
- [2] CLEO Collaboration, D. E. Jaffe *et al.*, Phys. Rev. D **62**, 072005 (2000).
- [3] M. Zoeller, Ph.D. thesis, State University of New York, Albany, 1994 (unpublished).
- [4] I. Dunietz, Phys. Rev. D **58**, 094010 (1998).
- [5] CLEO Collaboration, G. Crawford *et al.*, Phys. Rev. D **45**, 752 (1992).
- [6] A. Rubiera, Ph.D. thesis, U. of Florida [UF-IHEPA-00-01, hep-ex/0011066].
- [7] CLEO Collaboration, Y. Kubota *et al.*, Nucl. Instrum. Methods Phys. Res., Sect. A **320**, 66 (1992).
- [8] R. Brun *et al.*, GEANT v.3.15, CERN DD/EE/84-1 (unpublished).
- [9] T. S. Hill, Nucl. Instrum. Methods Phys. Res., Sect. A **418**, 32 (1998).
- [10] CLEO Collaboration, L. Gibbons *et al.*, Phys. Rev. D **56**, 3783 (1997).
- [11] Particle Data Group, Eur. Phys. J. C **3**, 1 (1998).